Site Description

Climate The mean annual air temperature (1980-2005) was -1.0 ºC in Healy, Alaska and the mean annual precipitation was 390 mm. During the study period, (spring 2004-winter 2006-07), annual air temperature was cooler than the mean by 1-2 ºC. Annual precipitation was greater in 2005 (540 mm) and 2006 (472 mm) than the long-term average, but was less in 2004 (324 mm). Permafrost temperatures have been monitored in a 30 m deep borehole in the study area since 1985 (maximum temperature range = -0.7 to -1.2 ºC at 10 m during mid-August)[1]. During this time frame, researchers recorded rapidly increasing deep permafrost temperatures (by ~0.7 ºC at 10 m) from 1990 until 1998, followed by a more recent slight cooling (by ~0.15 ºC) between 1998 and 2004[2].

Soils and Geography The study site was located (63°52'42"N, 149°15'12"W) at 700 m elevation on a gently sloping (~4%), north facing glacial terminal moraine that dates to the Early Pleistocene[3]. An organic horizon, 0.45-0.65 m thick, covers cryoturbated mineral soil that is a mixture of glacial till (small stones and cobbles) and windblown loess. Soil organic pools to 1-meter depth averaged 59.8 ± 2.8 kg C m^{-2} across all three sites. Permafrost was found within one meter of the soil surface, and therefore the soils were classified in the soil order Gelisol[4]. This watershed is in the southern half of the permafrost zone and thus may be especially sensitive to the changes in regional climate that have been documented over the past several decades[2]. Indeed, similar permafrost

thaw features occur on adjacent hill slopes and across the wider northern foothills area of the Alaska Range[5].

Plot Locations and Vegetation Our minimal thaw site had the shallowest summer thaw depth and the least ground surface subsidence, and the vegetation was typical moist acidic tundra[6], dominated by the tussock-forming sedge, *Eriophorum vaginatum*, with coexisting deciduous and evergreen shrubs, and an understory of mosses and lichens[7]. A second site, located adjacent to the borehole, had moderate summer thaw depths and increased ground subsidence[8]. Here the vegetation composition was similar to our minimal thaw site, but with increased biomass of all plant groups. Lastly, an extensive thaw site was located in an area where permafrost degradation had occurred at least several decades prior to the establishment of the borehole; thermokarst can already be observed in air photos of the area taken in 1954. This site had the deepest summer thaw depth and the most ground subsidence, and the plant biomass has shifted to dominance by shrubs, including blueberry (*Vaccinium uliginosum)* and cloudberry (*Rubus chamaemorus)*, at the expense of sedges (Supplementary Fig. 2).

Carbon Flux Measurements

Growing Season The difference between gross primary production (GPP) and ecosystem respiration (R_{eco}) equals the net ecosystem exchange (NEE) of C. Each of these components of ecosystem C exchange was either directly measured (NEE, R_{eco}) or indirectly estimated (GPP). We used closed chambers rather than an eddy covariance tower because in our study area, permafrost thaw and thermokarst depressions occurred

at a smaller spatial scale than what could be resolved with an eddy covariance footprint[9]. At each site, NEE was estimated at six locations spaced 8 m apart along a 40 m transect. In the summer of 2003, two square plastic bases (70x70 cm) were cut into the soil organic layer to a depth of ~5cm. The bases were subsequently used to seat a clear acrylic chamber that was 40 cm high, a height that fully accommodated the tallest plants. The two chamber bases in each location were treated as one replicate, for n=6 replications per site. At each site, the chamber bases spanned the range of microtopography created by thermokarst depressions. During measurements, a clear chamber was firmly fixed to the base but not sealed airtight, thereby minimizing the pressure differentials that can affect flux measurements[10]. In 2004, we only used a single chamber that was moved among chamber bases and sites, while in 2005 and 2006, we used both an automated system along with periodic manual measurements. Side by side comparisons showed no difference between the methods for flux calculation. For the autochamber system, R_{eco} was measured only at night (photosynthetically active radiation (PAR)<5 μmole m^{-2} s^{-1}). For the static chamber, R_{eco} was also measured during the daytime by placing an opaque cloth over the top of the chamber to stop photosynthetic uptake.

For all static and auto chamber measurements, air was circulated between the chamber and an infrared gas analyzer (LI-800, LICOR Corp., Lincoln, Nebraska) at 1 L min^{-1} for 1.5 minutes and the CO_2 concentration measured at 2-second intervals. For the static measurements, CO_2 concentrations were recorded to a Palm (Sunnyvale, CA) Tungsten C portable computing device using the software program Online (Conklin Systems, Eaton Rapids, MI). For the automated system, the LI-800 data was recorded on

a Campbell Scientific CR10X at 5-second intervals. Two small fans mixed the chamber air, while air temperature and relative humidity were recorded inside the chamber with a HOBO sensor (Onset, Pocasset, MA). For the static chamber measurements, PAR was measured inside the chamber with a LICOR quantum sensor attached to a LI-1400 data logger. For the automated chamber, PAR was recorded at a weather station 50-400 meters from the sites. A correction factor (19% reduction) was developed from simultaneous measurements of chamber and weather station PAR to account for the effect of reduced light transmission by the acrylic, and light interception by the chamber support structures. In conjunction with flux measurements, the thickness of unfrozen ground (seasonal thaw layer) was measured once per week at each chamber base.

Gas flux measurements generally began immediately after snowmelt and continued until snowfall in September to describe the entire growing season. To describe daily and weekly environmental and gas exchange variability, in 2004 we conducted static chamber measurements 5 times per week at 5 different times of day (pre-6 am, 9 am to noon, noon to 3 pm, 5 pm to 8 pm, and after 11 pm). Variability in incoming PAR was also created by artificially reducing PAR to approximately one-half and one-quarter of ambient conditions with mesh screens placed entirely over the chamber during the mid-morning and late afternoon measurements. This standard methodology was used in developing light response curves in order to interpolate between measurement points using environmental data. Static chamber measurements were continued in 2005 and 2006, but in these years measurements were only conducted three times of day (approximately 9 am to noon, 2 pm to 6 pm, and after 7 pm) because the automated chamber system was also collecting gas exchange measurements. The automated

chamber system was moved every 7-12 days among the three sites, and in general, measured continuously for at least 3 days in a given location.

Winter After the first snowfall, C exchange measurements were continued on the snow surface (Oct 2004-March 2005), and in snow pits dug to the soil surface (November 2005-April 2007). Snow surface measurements were only made when the wind was calm (< 0.2 m/s) because wind can evacuate CO_2 from the snow profile, resulting in artificially low or highly erratic efflux rates[11]. A rectangular chamber (22.5 x 35.3 cm^2) was pressed into the snow surface to create an imprint, lifted briefly to flush the chamber, and replaced in the imprint. Chamber CO_2 concentration was measured for 6 minutes, and snow depth was recorded. In 2005-2006, a new method was adopted because it was less sensitive to wind conditions[12]. Snow pits were dug between 0.15 and 0.75 m in depth, leaving ~5 cm of residual snow on the ground surface. Using the same approach as the snow surface measurements, an imprint in the residual snow was used to create a seal with the edge of the chamber. In addition, the outside edge of the chamber was covered with a thin layer of snow. We determined that 13-15 minutes were necessary for CO_2 efflux to approach a near constant rate after the snow pit was excavated, similar to previous findings[12]. Six locations were measured adjacent to the chamber base locations for each site. Care was taken to avoid the established chamber bases in order to preserve the thermal insulating properties of the snow cover on the long-term monitoring collars. Winter measurements were limited due to harsh field conditions where air temperature routinely fell below -20°C. Over the study period, each site was successfully sampled on 19 separate days distributed evenly over the winter months, for a total winter data set of

nearly 200 individual flux observations. While the total number of observations are much lower than those made during the growing season, the flux variability is also lower in wintertime due to fewer respiration sources and our measurements fall within the normal range reported for winter flux from other northern sites[11,13,14].

Annual Carbon Balance Calculation

Seasonal and annual estimates of C balance were estimated using two methods: gap filling with response functions to environmental factors, and by interpolating mean estimates between time points. Both methods were applied during different parts of the growing season because R_{eco} and NEE in the months of May and September were difficult to explain with response functions, likely because plant phenology and soil conditions were changing rapidly at those times of year. For June-August, a hyperbolic equation was used to describe the relationships between PAR and NEE[15]. For R_{eco}, we used the nighttime and darkened-chamber measurements to develop exponential relationships between R_{eco} and air (June-August) or soil temperature (winter, and June-August 2006). During the shoulder seasons in spring and fall, integrated estimates of NEE and R_{eco} were developed by interpolating fluxes between time points. We defined the total growing season as being the period of May-September, but we note that snow often covered the site for the first few days of May and the last days of September. The total number of individual NEE and R_{eco} measurements used for making integrated growing season estimates were 2,986 in 2004, 5,148 in 2005, and 7,152 in 2006. GPP was estimated as the difference between the integrated NEE and R_{eco} values. Cross-site

patterns of increased GPP corresponded to direct measurements of aboveground net primary productivity (NPP) made at the same sites[7].

Growing Season Isotope Measurements

Field Ecosystem respiration $^{14}C/^{12}C$ and $^{13}C/^{12}C$ isotopic ratios were measured using a modified dynamic flow chamber system analogous to the system used for measuring ecosystem CO_2 fluxes[16,17]. In each site, permanent collars (25.4 cm dia.) remain inserted in the soil/moss surface adjacent to the C flux collars. At monthly intervals during the growing season (May-September), dark, 10L, plastic chambers were placed over the collars and air was drawn through an gas analyzer to determine the CO_2 concentration, then either through an Ascarite CO_2 scrubber or through a molecular sieve before returning to the chamber. To remove background CO_2 present when the chamber top was fit to the collar and collect respired CO_2 alone, the air stream was scrubbed with Ascarite. Fluxes were determined by monitoring the rise in CO_2 concentration in the closed chamber-sampler system, and the airflow (thus scrubbing rate) was adjusted to maintain system CO_2 levels at, or slightly above, ambient soil surface conditions. Carbon dioxide was scrubbed from the system at a rate similar to that of soil CO_2 efflux until 2-3 chamber volumes of air had passed through the scrubber, when the CO_2 remaining is almost exclusively soil-respired CO_2. The air stream was then diverted through a molecular sieve (13X) to quantitatively trap CO_2 until 1.0 mg of CO_2-C was adsorbed. In the laboratory, the molecular sieve traps were heated to 625°C to desorb CO_2[18]. Carbon dioxide was then purified and analyzed for $\delta^{13}C$ and $\Delta^{14}C$. The $^{13}C/^{12}C$ isotopic ratios

were used in the final analysis to correct for incomplete scrubbing in the chamber-sampler system.

Laboratory To estimate the contribution of plant respiration, surface litter, and deep, old soil C to surface $\Delta^{14}CO_2$ fluxes, we incubated these materials in the laboratory to determine the isotopic composition of evolved CO_2[19,20]. In 2004, we collected 2 replicate soil samples per site down to the mineral soil interface (typically the full August active layer depth) and separated the profiles into 5 depth increments (0-5, 5-15, 15-25, 25-35, 35+ cm). The final depth increment was variable because the total organic layer thickness varied among samples. All samples were split, large roots and stems gently removed while minimizing disturbance, and the halves kept relatively intact to preserve the soil structure. Soil core splits were incubated in separate glass jars at 3°C and 8°C to determine the temperature sensitivity for respiration from these soils in order to account for soil temperature gradients that occur in the field (see next section)[21]. Rates of CO_2 production were then measured daily using a gas analyzer to monitor the change in CO_2 concentration in the incubation jar headspace over time. Jars were sealed and flushed with moist CO_2-free air when CO_2 concentrations exceeded 1%. Since field experiments have shown a drop in soil respiration fluxes of ~50% within 3-5 days after tree girdling in a high latitude forest[22], we used that as an estimate of the length of time required for any remaining small roots plus mycorrhizae to deplete a large proportion of their labile C reserves and thus contribute relatively little to CO_2 flux[20,23]. Carbon dioxide respired from the incubation after this initial period is thought to be dominated by heterotrophic decomposition of soil organic matter. After 5 days of incubation in the laboratory, the

jars were completely scrubbed with CO_2-free air, and respired $^{14}CO_2$ was allowed to accumulate. Carbon dioxide in the jar headspace was then collected from the 8°C incubation for $\Delta^{14}C$ analysis. Similar incubations were made of aboveground and belowground plant parts harvested from 5x5 cm quadrats during the growing season. Live plant parts were separated and roots were rinsed with deionized water and incubated for 4 hours in separate, CO_2-free air flushed jars. After that time, CO_2 was collected and prepared for isotopic analysis as described above.

Isotope Partitioning Calculations

End members We estimated the relative contribution of the plant and soil components to the R_{eco} flux using the $\Delta^{14}C$ measurements and a standard statistical modeling approach[24,25]. The laboratory soil incubations were combined into surface soil (top 2 layers) and deep soil (lower 3 layers) components by flux-weighting the soil incubations. To calculate a combined isotope respiration value for the surface and deep soil, the $\Delta^{14}C$ values for the layers that were combined were weighted by three factors simultaneously: 1) the relative CO_2 flux on a per gram dry soil basis, 2) the relative amount of soil mass in the combined horizons, and 3) by the average field temperature for the horizons (this varied over the season) (Table S4).

The soil incubations were conducted in 2004, so to partition the field R_{eco} $\Delta^{14}C$ values in 2005 and 2006, we estimated the expected change in the soil respiration $\Delta^{14}C$ values using a two-pool model[26]. The atmospheric $\Delta^{14}C$ decline of ~5‰ yr^{-1} is an upper bound for changes in soil respiration that must be declining more slowly due to the longer residence time of C in plants and soil. The two-pool model needed two estimated

parameters for each individual incubation layer: 1) the relative proportion of C in each of two pools, and 2) the turnover time of the two pools, assuming that one pool is relatively fast and one is relatively slow. These assumptions are based on the fact that soil organic matter is heterogeneous and comprises more than one pool. Because the incubations utilized only the organic layer, a recalcitrant third pool, such as might be associated with mineral soils, was not necessary. Sensitivity analyses showed that setting the faster turnover time pool anywhere from 1-3 years to represent labile C inputs did not affect the overall estimated $\Delta^{14}C$ value for 2005 and 2006, so we chose a two year turnover time to represent the combined residence time in plants and soil before decomposition of the faster pool. Knowing the size of the C pool in each layer and defining the turnover time as 2 years constrains the relative proportion of C that can be contained in this pool to <10%; the upper limit being set by the total incoming NPP. Based on these constraints, we set the relative proportion of this fast pool to be 10% for the surface layer, and divided that in half for every subsequent layer deeper in the profile to reflect the attenuation of labile C transport deeper in the soil profile. As a result, this fast pool was ~1% of the total C by the 25-35 cm layer. Using this model, we predicted that soil incubation $\Delta^{14}C$ values, if measured in 2005 and 2006, would have declined anywhere from 0-1‰ per year from 2004 $\Delta^{14}C$ values, depending on the individual layer. This effect is negligible over the time frame of this project; the precision of the accelerator mass spectrometer is on the order of 2-3‰ for individual samples. Plant respiration $\Delta^{14}C$ values measured over the growing season (data not shown) matched the atmospheric values in 2004, and were assumed to follow the atmospheric decline measured for 2005 and 2006 (Fig. 2).

Statistical Partitioning Total R_{eco} $\Delta^{14}CO_2$ flux is a combination of surface and deep soil respiration, along with plant respiration. Because there is no single solution that describes the contribution of three unknown sources with a single isotope tracer, a standard statistical approach yields a range of possible contributions of the component sources to R_{eco}[24,25]. Of the sources (plant respiration, surface soil respiration, deep soil respiration), the contribution of the deep soil is the most constrained by the data, as demonstrated by the smallest standard deviation and overall range (Table S5). This is a result of the deep soil having a $\Delta^{14}C$ value furthest away from the $\Delta^{14}C$ value of R_{eco}, thus its contribution to the total is most constrained. While the deep soil C was the only source that could bring the R_{eco} $\Delta^{14}C$ value below that of the ambient atmosphere, the $\Delta^{14}C$ values of plant respiration and surface soil respiration were at or above the atmospheric value and thus could substitute for one another. We tested the sensitivity of the statistical partitioning to changes in the deep soil $\Delta^{14}C$ value because it was influential for bringing the total ecosystem respiration isotope value below that of the atmosphere. To do this, the lower depth of all profiles was standardized to 35 cm to eliminate difference in overall organic layer depth among soil samples and sites. In this sensitivity analysis, eliminating the deepest incubated soils, thus increasing the deep soil $\Delta^{14}C$ value, had the effect of more than doubling the estimated proportion of deep C loss at the extensive site, while the moderate and minimal thaw site increased by 33% and 14% respectively. The estimated amount of deep soil C loss across sites in this sensitivity analysis was highly correlated with our original estimates (r=0.930), however the old C for some sites in some months became the dominant source and is thus likely overestimated by this sensitivity analysis.

Differences in old C loss across the permafrost thaw gradient resulted from a combination of proportionally higher old C losses and more total R_{eco} from sites with more thaw. There are several lines of corroborating evidence to support the idea that the mean predicted contributions from the statistical partitioning provide a reasonable picture of old C losses across sites. First, old C is predicted to be a relatively small proportion of total R_{eco} (3-year average of 8%-16% across sites). This predicted slow loss of old C is consistent with the recalcitrant nature of soil organic matter deeper in the soil profile. Second, the overall interannual decline in the R_{eco} $\Delta^{14}C$ values by ~9‰ (June-Aug average across sites) from 2004 to 2006 suggests that most, but not all, of the substrate that fuels R_{eco} has a fast turnover time of 1-2 years. This inferred turnover time is consistent with plant respiration and labile soil C pools as the major contributors to R_{eco}, while old C deep in the soil slowly decomposes. Lastly, as detailed in the main text, there is a high correlation between the proportion of old C loss and total ecosystem respiration across the sites.

Winter Isotope Measurements

The contribution of old C to winter respiration is less certain due to the difficulty of measuring surface isotope fluxes when overall C efflux rates were so low. Old C loss estimates made from soil profile $\Delta^{14}CO_2$ measurements in the field combined with the soil laboratory incubations suggest an increasing proportional contribution of old C from fall into winter that changes in parallel with the freeze-up of surface soil, and a decrease in overall R_{eco} over the same time period (Fig. S6; Table S6). Including the winter

fluxes increases old C contribution to total annual R_{eco} at all sites, and reinforces the general pattern across sites of increasing old C loss with increased permafrost thaw.

Field Because winter surface CO_2 fluxes are generally low and measurement conditions are challenging, isotope ratios were measured in the soil profile from permanently installed soil gas wells where CO_2 concentrations were higher. Soil pore space CO_2 was measured in gas sampling wells that have been installed at multiple depths in the soil profile (average sampling depth = 10-15 cm) at replicate locations per site (average number of unfrozen wells per site = 2-3). Stainless steel tubing, perforated and covered with mesh at the bottom, extends aboveground to fittings with gas-tight stopcocks. Air within the tubing equilibrates with soil pore CO_2 concentrations and was sampled at several intervals during the winter months over the three-year period. Air was pumped from the well at 0.25L/min for 1 minute through a molecular sieve as described for the ecosystem respiration measurements. The traps were returned to the lab and analyzed for $\delta^{13}C$ and $\Delta^{14}C$. The $^{13}C/^{12}C$ isotopic ratios measured on the traps are used in the final analysis to correct for any bulk air movement as a result of the pumping process.

The same gas wells are useful for illustrating the fingerprint of old C decomposition during the growing season. Decomposition of old C is a relatively small component of total R_{eco}, but is more prominent in measurements of soil profile CO_2 that are themselves a mixture of the same three sources in different proportions. Soil profile $\Delta^{14}CO_2$ was always below atmospheric values, with average values ranging as low as -224‰ for some sites in some months, and single observations as low as -397‰ recorded at the extensive thaw site. The ages of this C, expressed in radiocarbon years, are 1990

years and 4020 years old respectively, but in actuality represent a mixture of plant root respiration, and decomposition of recent detritus and old C that itself must be older than the mean age reported above, with the exact age of the old C depending on the relative proportions of these sources.

Analytical Partitioning In winter, ecosystem respiration is derived from only two sources (surface and deep soil) because plant respiration is minimal or absent. Ecosystem respiration isotope values in the late fall and winter are then a combination of CO_2 derived from surface soil and deep soil as the seasonal active layer refreezes both from the top down and the bottom up. We used the isotope value of surface and deep soil respiration as end-members in a two pool mixing model. From the model, we calculated the proportional contribution of deep soil respiration to total soil respiration. To estimate the error for partitioning, we used a mass balance method to account for variation in both the isotopic value of the soil respiration, and the variation of the isotopic composition of the end-members[27]. This method uses the standard deviation of the isotopic observations in combination with the number of replicates in order to calculate an error term for the partitioning calculation. Our winter measurements are few due to the extreme conditions, thus we pooled our estimates across sites and years to estimate an average proportion of wintertime old C loss. When the proportional old C loss for winter was combined with winter flux measurements and with the estimate of growing season old C loss, we calculated the three-year average annual old C flux to be 66 g C m^{-2} in the minimal thaw site, 93 g C m^{-2} yr^{-1} at the moderate thaw site, and 118 g C m^{-2} yr^{-1} at the extensive thaw site. The correlation between annual R_{eco} and annual proportion old C flux (R^2=0.92)

was similar to that of the growing season showing that sites with high proportion old C flux had high ecosystem respiration.

Soil Carbon Loss Calculations

Carbon loss projections are based on the assumption that the observed three-year average fluxes are representative of longer time periods, and can be extrapolated into the future. The 15-year thawing history of the moderate thaw site has been documented directly with the borehole temperature, while the extensive thaw site is a minimum of 55 years old (based on air photos), and likely to be less than 150 years old based on vegetation patterns at this site and the chronology of other thaw sites in Interior Alaska[28]. The range of C accumulation and loss estimates were based on the assumption of linear increases or decreases in C fluxes through time to connect observed site fluxes in the various stages of thaw. Two sets of scenarios were constructed that assumed that current flux measurements at the extensive thaw site were still not in equilibrium with increased surface soil accumulation from greater plant productivity. The first set of scenarios assumed that the average NEE at the extensive thaw site would stabilize at -52 g m^{-2} yr^{-1} (a conservative projection since this estimate excludes deeper thawing in the future) once the surface soil respiration re-equilibrates with increased inputs. This number is the average difference between the annual deep soil C loss at the extensive thaw site compared to the reference minimal thaw site. The current three-year average NEE at the extensive site is 38% lower than this estimated equilibrium value. The second set of scenarios assumed that the extensive thaw NEE would stabilize at -69 g m^{-2} yr^{-1}, where the additional 17 g m^{-2} yr^{-1} compensates for currently observed minimal thaw site C loss

that itself is likely the result of warming-induced changes at this least subsided site. This offset acknowledges that no site in this area is unaffected by regional warming, and that even the deep C loss rates at the minimal thaw site are likely to be currently above the long-term background rates. Each set of scenarios allowed the age of the extensive thaw site to vary from 55 years (in 2005) to 155 years, and future C losses were projected to 2099. Overall, varying the age of the extensive thaw site had a smaller effect on projected C loss compared to the differences in estimated long-term C loss rate. For the first scenario set, the range of projected C losses was 4.4-4.8 kg m^{-2}, with the lower end of the range using the older estimated age of the extensive thaw site. For the second scenario set, the range of projected C losses was 4.8-6.0 kg m^{-2}. These values represent a minimum loss because they are based on current thaw depths, which could be expected to increase with future warming.

It is important to note that while projecting current rates from our sites over a century constrains surface soil C gains and losses, it is not equivalent to total permafrost C emissions. Our observations do not account for future thawing and active layer thickening that will expose a larger pool of permafrost C to decomposition. Also, net exchange of CO_2 does not account for hydrologic C losses or methane emissions. Preliminary estimates of such losses for the Eight Mile Lake watershed could increase ecosystem C loss rates by an additional ~10-15%. And lastly, we don't know the true range of interannual C flux variability over long time scales; C loss rates at the extensive site were double in 2004 and 2005 compared to the three-year average. With only three years of observations, it is difficult to disentangle the cause of this interannual variability. In 2006, positive NEE values were the result of slightly higher GPP and slightly lower

R_{eco}, but no obvious environmental factors explained this variation making it difficult to determine the likely frequency of NEE values over longer time periods. In summary, these unknowns are largely expected to make future C losses larger, thus our projections of the future are conservative.

Extrapolating the loss rate from this site to the global surface permafrost C pool cannot be considered a true projection, since this site does not provide any information about the rate of thawing on a pan-Arctic scale. Also, it is known that upland and lowland sites may differ in the release rate of CO_2 and methane (CH_4), depending on whether aerobic or anaerobic decomposition predominates[29,30]. While these gases have different greenhouse warming potentials (GWP), recent calculations have suggested that the overall climate effect of thawed permafrost C decomposition is actually similar between aerobic versus anaerobic environments[31]. This is because total C emissions are lower from anaerobic environments, but are compensated by the higher GWP of methane. Here we have extrapolated our upland site to the global permafrost C pool to determine potential C emissions, which assumes that C dynamics at this site are similar elsewhere. If anaerobic conditions are more typical in lowland landscapes, then our estimate will have overestimated total C emissions to the atmosphere, but will still accurately account for the climate impact of permafrost thaw. Therefore, using rates from this site presents an emissions estimate in CO_2-equivalents. Lastly, we used the value of 818 Pg C contained in the top 3 m of soil orders that contain permafrost. This is less than the total soil C pool in the permafrost zone including soil orders that do not have permafrost (1218 Pg C). Soil orders without permafrost are likely to also lose C, but we do not include that in our estimate in order to be conservative.

Citations

1 Osterkamp, T. E. and Romanovsky, V. E., Evidence for warming and thawing of discontinuous permafrost in Alaska. *Permafrost Periglacial Process*. **10** (1), 17-37 (1999).

2 Osterkamp, T. E., Characteristics of the recent warming of permafrost in Alaska. *Journal Of Geophysical Research-Earth Surface* **112** (F2) (2007).

3 Wahrhaftig, C. , edited by U.S. Geological Survey (1958), pp. 1-68.

4 USDA Soil Conservation Service, Soil Survey Staff, edited by Natural Resources Conservation Service (USDA, Washington, DC, USA, 1999), Vol. Agricultural Handbook 436.

5 Yocum, L.C., Adema, G.W., and Hults, C.K., presented at the Proceedings of the central Alaska Park Sciences symposium, Denali Park, Alaska, 2006 (unpublished).

6 Epstein, H. E. et al., Detecting changes in arctic tundra plant communities in response to warming over decadal time scales. *Global Change Biology* **10** (8), 1325-1334 (2004).

7 Schuur, E. A. G., Crummer, K. G., Vogel, J. G., and Mack, M. C., Plant species composition and productivity following permafrost thaw and thermokarst in alaskan tundra. *Ecosystems* **10** (2), 280-292 (2007).

8 Osterkamp, T.E, The recent warming of permafrost in Alaska. *Global and Planetary Change* **49**, 187-202 (2005).

9 Vourlitis, G. L. et al., Physiological models for scaling plot measurements of CO2 flux across an arctic tundra landscape. *Ecological Applications* **10** (1), 60-72 (2000).

10 Lund, C. P., Riley, W. J., Pierce, L. L., and Field, C. B., The effects of chamber pressurization on soil-surface CO2 flux and the implications for NEE measurements under elevated CO2. *Global Change Biology* **5** (3), 269-281 (1999).

11 Vogel, J. G., Valentine, D. W., and Ruess, R. W., Soil and root respiration in mature Alaskan black spruce forests that vary in soil organic matter decomposition rates. *Canadian Journal of Forest Research* **35** (1), 161-174 (2005).

12 Grogan, P. and Jonasson, S., Ecosystem CO2 production during winter in a Swedish subarctic region: the relative importance of climate and vegetation type. *Global Change Biology* **12** (8), 1479-1495 (2006).

13 Fahnestock, J. T. et al., Winter and early spring CO2 efflux from tundra communities of northern Alaska. *Journal of Geophysical Research-Atmospheres* **103** (D22), 29023-29027 (1998).

14 Oechel, W. C. et al., Acclimation of ecosystem CO2 exchange in the Alaskan Arctic in response to decadal climate warming. *Nature* **406** (6799), 978-981 (2000).

15 Thornley, J.H.M. and Johnson, I.R., *Plant and crop modeling: a mathematical approach to plant and crop physiology*. (Oxford, (UK): Clarendon., 1990).

16 Gaudinski, J.B., Trumbore, S.E., Davidson, E.A., and Shuhui, Z., Soil carbon cycling in a temperate forest: radiocarbon-based estimates of

residence times, sequestration rates and partitioning of fluxes. *Biogeochemistry* **51**, 33-69 (2003).

17 Norman, J.M. et al., A comparison of six methods for measuring soil-surface carbon dioxide fluxes. *Journal of Geophysical Research* **102** (D24), 28,771-728,778 (1997).

18 Bauer, J., Williams, P.M., and Druffel, E.R.M., Recovery of sub-milligram quantities of carbon dioxide from gas streams by molecular sieve for subsequent determination of isotopic natural abundance. *Analytical Chemistry* **64**, 824-827 (1992).

19 Cisneros-Dozal, L.M., Trumbore, S., and Hanson, P.J., Partitioning sources of soil-respired CO2 and their seasonal variation using a unique radiocarbon tracer. *Global Change Biology* **12** (2), 194-204 (2006).

20 Schuur, E. A. G. and Trumbore, S. E., Partitioning sources of soil respiration in boreal black spruce forest using radiocarbon. *Global Change Biology* **12** (2), 165-176 (2006).

21 Dutta, K., Schuur, E. A. G., Neff, J. C., and Zimov, S. A., Potential carbon release from permafrost soils of Northeastern Siberia. *Global Change Biology* **12** (12), 2336-2351 (2006).

22 Högberg, P et al., Large-scale forest girdling shows that current photosynthesis drives soil respiration. *Nature* **411** (6839), 789-792 (2001).

23 Carbone, M. S., Czimczik, C. I., McDuffee, K. E., and Trumbore, S. E., Allocation and residence time of photosynthetic products in a boreal forest using a low-level C-14 pulse-chase labeling technique. *Global Change Biology* **13** (2), 466-477 (2007).

24 Phillips, D. L. and Gregg, J. W., Source partitioning using stable isotopes: coping with too many sources. *Oecologia* **136** (2), 261-269 (2003).

25 Schuur, E. A. G., Trumbore, S. E., Mack, M. C., and Harden, J. W., Isotopic composition of carbon dioxide from a boreal forest fire: Inferring carbon loss from measurements and modeling. *Global Biogeochemical Cycles* **17** (1), - (2003).

26 Trumbore, S., Age of soil organic matter and soil respiration: radiocarbon constraints on belowground C dynamics. *Ecological Applications* **10** (2), 399-411 (2000).

27 Phillips, D. L. and Gregg, J. W., Uncertainty in source partitioning using stable isotopes. *Oecologia* **127** (2), 171-179 (2001).

28 Jorgenson, M. T., Racine, C. H., Walters, J. C., and Osterkamp, T. E., Permafrost degradation and ecological changes associated with a warming climate in central Alaska. *Climatic Change* **48** (4), 551-579 (2001).

29 Christensen, T. R. et al., Thawing sub-arctic permafrost: Effects on vegetation and methane emissions. *Geophysical Research Letters* **31** (4), - (2004).

30 Walter, K. M. et al., Methane bubbling from Siberian thaw lakes as a positive feedback to climate warming. *Nature* **443** (7107), 71-75 (2006).

31 Schuur, E. A. G. et al., Vulnerability of permafrost carbon to climate change: Implications for the global carbon cycle. *Bioscience* **58** (8), 701-714 (2008).

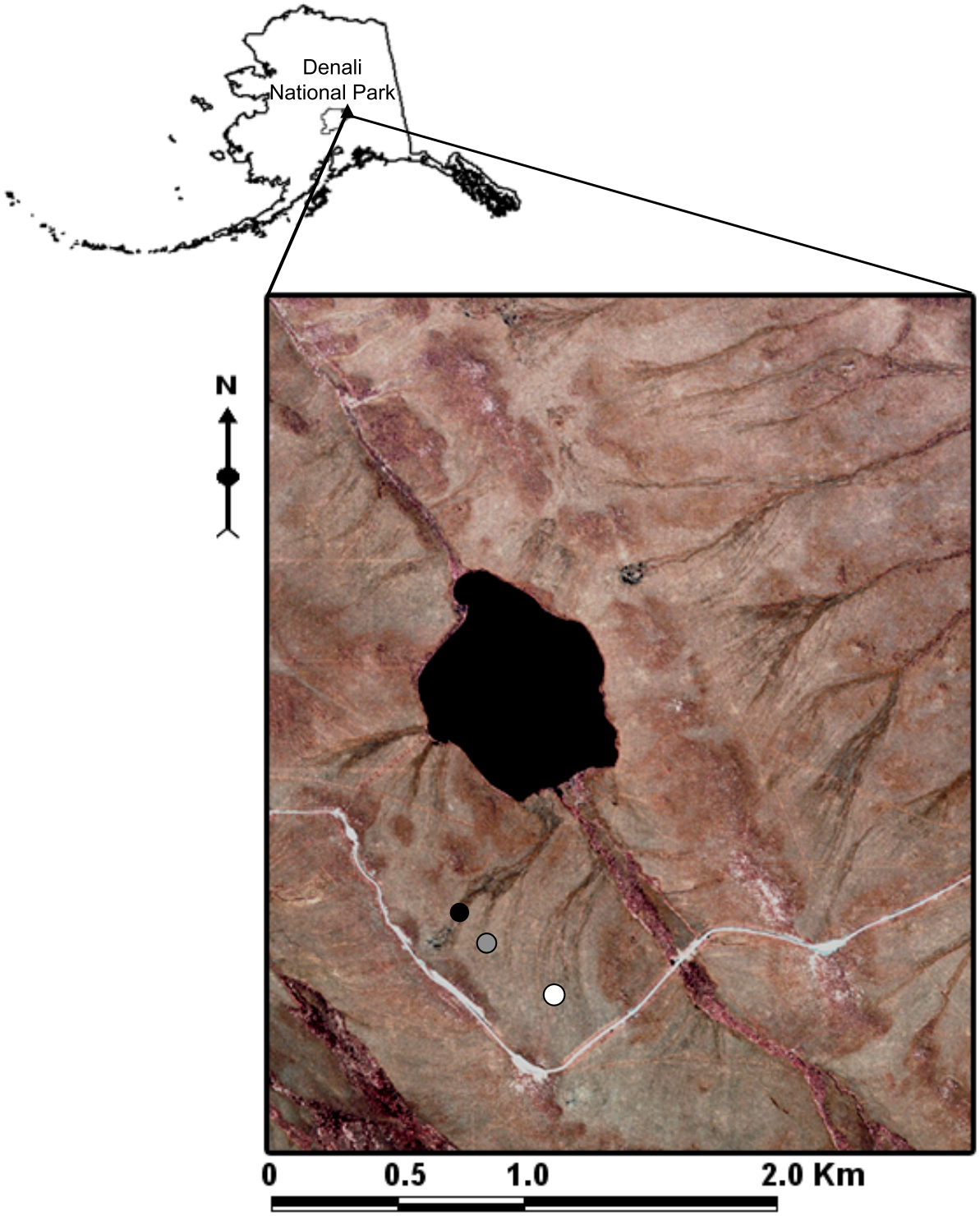

Supplementary Figure 1. The state of Alaska and the outline of Denali National Park, with an infrared air photo inset of the Eight Mile Lake study site and surrounding area. Ground subsidence as a result of permafrost thaw and ice wedge melting is visible as dark striations that occur at the study site and the surrounding hillslopes. Symbols represent the location of the extensive thaw site (black), the moderate thaw site adjacent to the borehole (grey), and the minimal thaw site (white).

Supplementary Figure 2. Early-season photo of extensive permafrost thaw showing ground subsidence and water ponding (top). Due to the shallow thaw at this time of year, the water table is still visible at the soil surface. During mid-season (bottom), the water table drops below the soil surface as the seasonal thaw depth increases. Tundra dominated by shrubs following permafrost thaw is visible in the foreground; minimally-subsided tundra dominated by the tussock-forming sedge, *Eriophorum vaginatum*, is visible in the far background as the light green vegetation in the left middle of the photo.

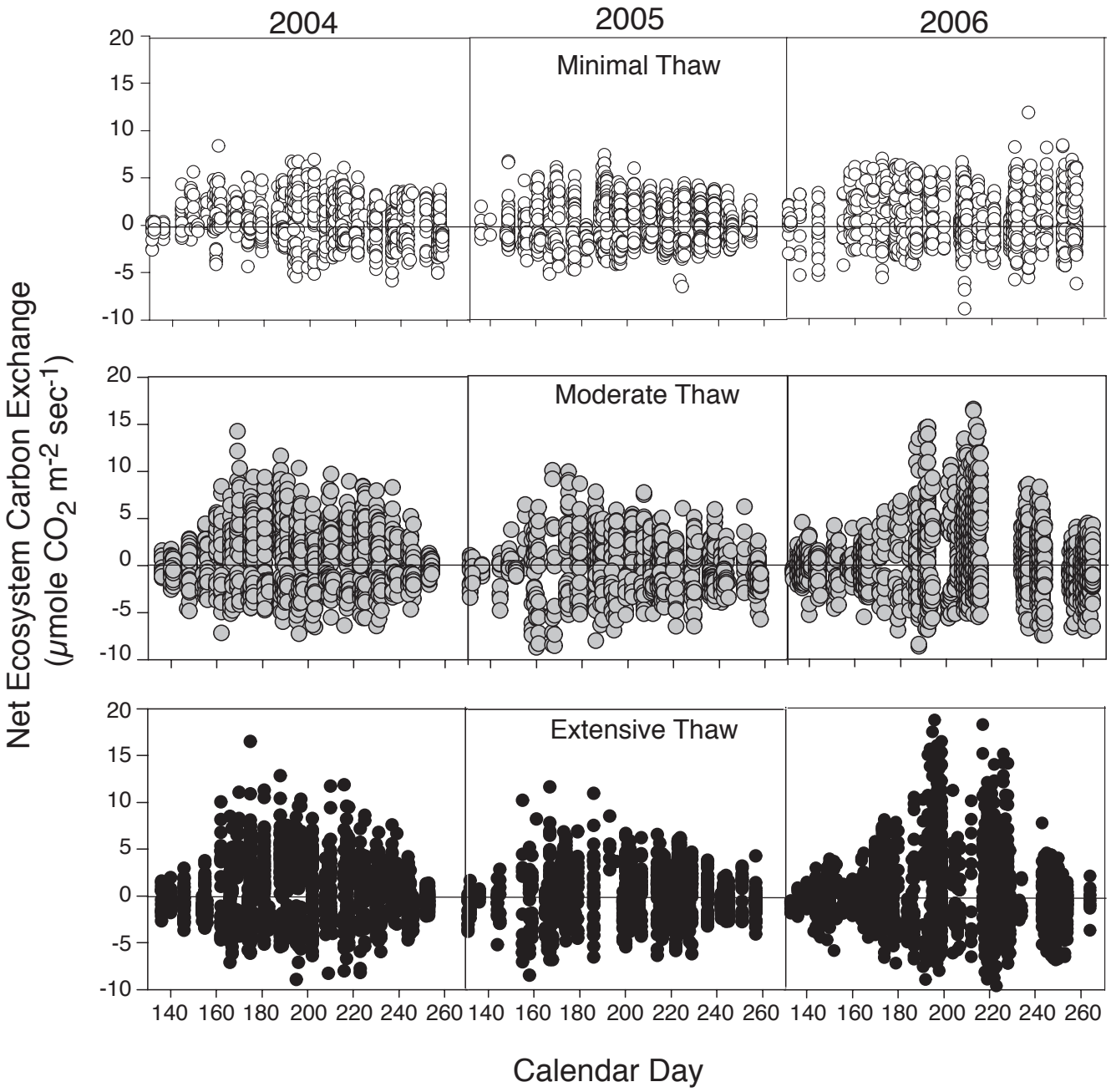

Supplementary Figure 3. All C exchange measurements made with static and autochambers during the growing season over the three-year study period from 2004 to 2006. Positive numbers denote net ecosystem C uptake; negative numbers denote net ecosystem C loss.

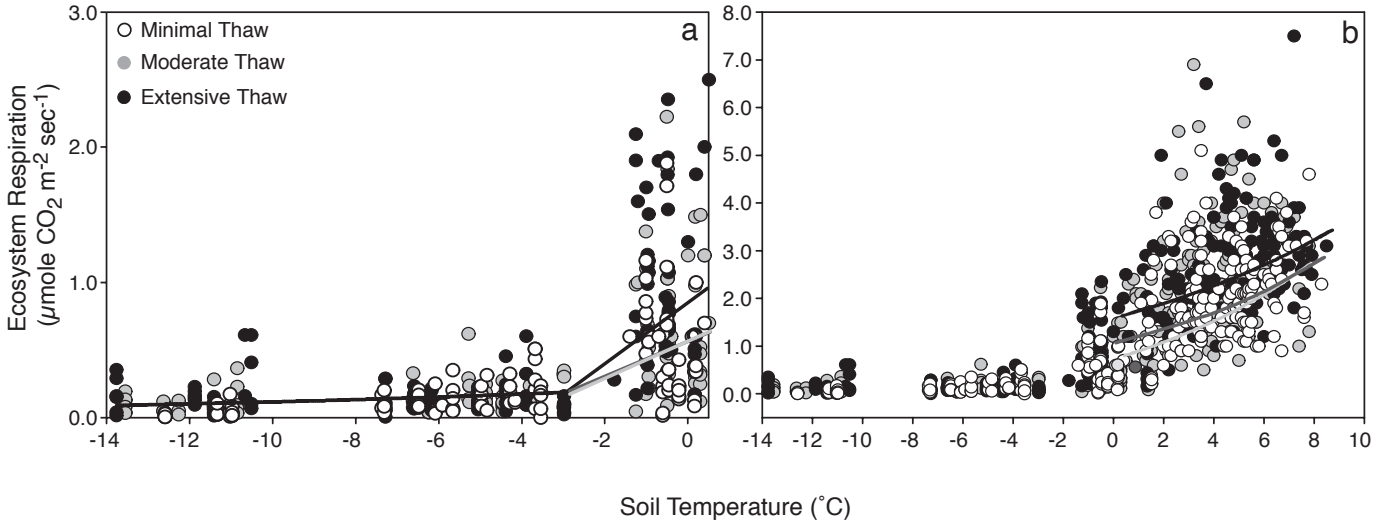

Supplementary Figure 4. Ecosystem respiration as a function of average integrated soil profile temperature (10-40 cm depth) for winter (a) and on an annual basis (b). Winter respiration measurements below -2°C were described by a single exponential relationship for all sites because there were no differences. Respiration measurements between -2ºC and 0ºC were described by site-specific lines; here the minimal and moderate lines overlap. Growing season respiration measurements above 0˚C show site-specific exponential relationships. The site-specific lines are shaded black (extensive), dark grey (moderate), and off-white (minimal) for clarity.

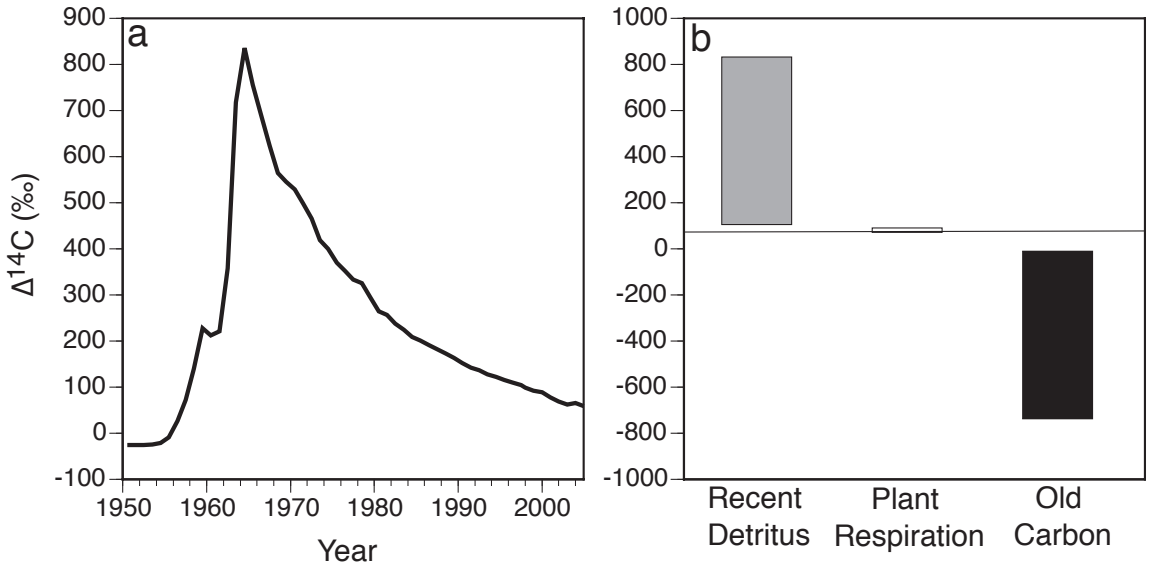

Supplementary Figure 5. Atmospheric $\Delta^{14}C$ approximately doubled five decades ago as a result of thermonuclear weapons testing (a). Possible sources of C to total ecosystem respiration differ in their potential $\Delta^{14}C$ values, shown as approximate ranges of possible values, with the atmospheric value (for 2005) shown as a horizontal line (b). Here, recent and old C are delineated in relation to the bomb $\Delta^{14}C$ peak, with positive bomb $\Delta^{14}C$ values defined as recent C. Old C is defined as pre-bomb C, spanning a period from 1950 to thousands of years, with the oldest possible ages corresponding to the Holocene accumulation of soil organic matter at this site. Plant respiration $\Delta^{14}C$ values are at, or slightly above, the current atmosphere due to the dominant influence of recent photosynthesis, and a smaller contribution from internal plant C storage pools. Old C is the only source pool below the current atmospheric $\Delta^{14}C$ value.

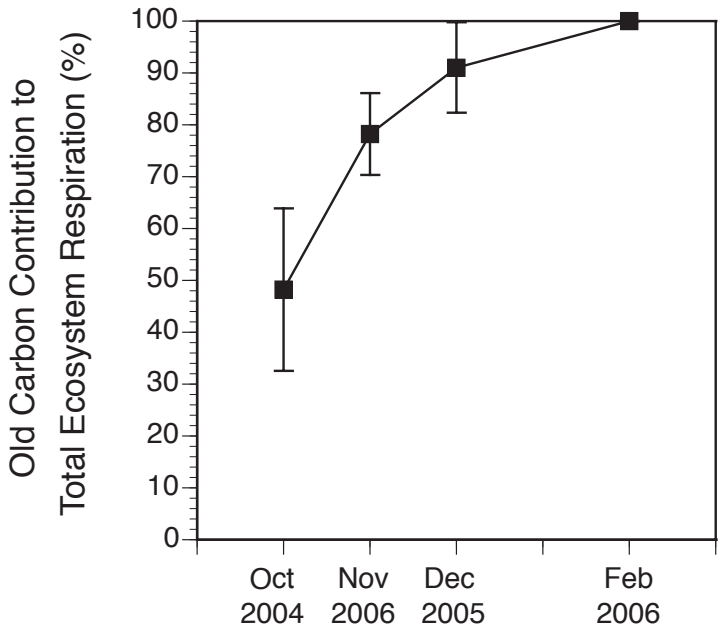

Supplementary Figure 6. The proportional contribution of old C to winter respiration for all winter months measured for isotopes during the 2004-2006 period (mean±SE). Because the total number of measurements was small due to low C flux rates and challenging measurement conditions, this estimate is presented as a mean across all sites. The standard error bars show the variability of site means.

Supplementary Table 1. Environmental and site characteristics for three sites that differ in the degree of permafrost thaw and extent of ground subsidence at Eight Mile Lake, Alaska. Mean (± SE) growing season soil temperature and active layer thickness (measured from current ground surface) for the three years of study. Microtopography data is reported as the standard deviation of microsite elevation detrended to remove the overall hillslope effect on elevation. The data set was truncated at the highest and lowest 5% of the data to remove outliers from the normalization procedure. Even on flat terrain, there is some microtopographical relief due to the presence of the *E. vaginatum* tussocks that rise ~20-30 cm above the moss surface; measurements greater than that are interpreted as additional ground subsidence due to ice wedge melting. The maximum depression depth is the average of the deepest 10% of the normalized microtopography measurements, using the top 10% at each site as a zero reference.

	Minimal Thaw	Moderate Thaw	Extensive Thaw
Soil Temperature (10 cm, ºC)	6.8±0.2	8.8±0.1	9.1±0.2
Active Layer Thickness (m)	0.69±0.02	0.70±0.02	0.78±0.05
Surface microtopography (m)	0.18	0.28	0.36
Maximum depression depth (m)	-0.67±0.005	-1.03±0.009	-1.30± 0.014

Supplementary Table 2. Growing season, winter, and annual estimates of gross primary productivity (GPP), ecosystem respiration (R_{eco}), and net ecosystem exchange (NEE). Negative values denote release to the atmosphere, while positive values denote net uptake by ecosystem. Values are the mean g C m^{-2} (± SE) of the integrated model estimates for n=6 locations per site. Different letters signify statistically significant differences across sites at p=0.05 when corrected for multiple comparisons.

		Growing Season			Winter	Annual	
Site	Year	GPP	R_{eco}	NEE	R_{eco}	R_{eco}	NEE
Minimal	2004	327±20^{a}	-287±12^{a}	40±16^{a}	-75±12^{a}	-362±17^{a}	-36±16^{a}
Moderate		445±48^{b}	-339±36^{ab}	105±26^{b}	-79±14^{a}	-418±39^{b}	26±26^{b}
Extensive		449±56^{b}	-403±37^{b}	46±23^{a}	-104±18^{b}	-507±41^{b}	-58±23^{a}
Minimal	2005	305±14^{a}	-276±13^{a}	29±4^{a}	-48±10^{a}	-324±16^{a}	-19±4^{a}
Moderate		383±34^{a}	-340±24^{ab}	43±24^{a}	-50±11^{a}	-390±26^{ab}	-7±24^{a}
Extensive		375±28^{a}	-393±36^{b}	-17±13^{b}	-61±16^{a}	-454±39^{b}	-78±13^{b}
Minimal	2006	329±24^{a}	-266±18^{a}	62±14^{a}	-57±11^{a}	-323±21^{a}	5±14^{a}
Moderate		430±51^{ab}	-313±30^{ab}	117±36^{a}	-60±12^{a}	-373±32^{ab}	57±36^{a}
Extensive		480±83^{b}	-359±58^{b}	121±31^{a}	-81±17^{b}	-440±61^{b}	40±31^{a}
Minimal	**Average**	320±19^{a}	-276±15^{a}	44±11^{a}	-60±11^{a}	-336±18^{a}	-17±11^{a}
Moderate		419±44^{b}	-331±30^{ab}	88±29^{b}	-63±12^{a}	-394±32^{b}	25±29^{b}
Extensive		435±56^{b}	-385±44^{b}	50±22^{ab}	-82±17^{b}	-467±17^{b}	-32±22^{a}

Supplementary Table 3. Two-way ANOVA testing annual differences in gross primary productivity (GPP), ecosystem respiration (R_{eco}), and net ecosystem exchange (NEE) with site and year as fixed effects.

	df	GPP		R_{eco}		NEE	
		F	p	F	p	F	p
Site	2, 45	6.70	<0.01	14.3	<0.01	5.11	0.01
Year	2, 45	1.47	0.24	2.86	0.07	7.79	<0.01
Site × Year	4, 45	0.86	0.97	0.1	0.97	1.38	0.27

Supplementary Table 4. Fluxes and isotopes of carbon dioxide from laboratory incubations of individual soil organic layers at 8°C. Values are means (± SE)

Site	Soil Layer cm	Carbon Flux μg C gdw^{-1} hr^{-1}	Soil Mass kgdw m^{-2}	Average Summer Temperature °C	$\Delta^{14}C$ ‰
Minimal Thaw	0-5	8.09±4.21	3.43±1.05	14.0	+107±22
	5-15	6.05±2.14	7.77±2.25	12.2	+69±13
	15-25	3.07±1.64	13.74±4.64	4.7	+27±2
	25-35	1.66±0.23	27.95±5.95	2.0	-21±5
	35+	1.26±0.65	101.43±29.09	0.6	-35±27
Moderate Thaw	0-5	7.65±1.31	3.80±0.56	14.0	+94±11
	5-15	3.47±1.73	5.49±1.01	12.2	+79±23
	15-25	3.16±0.71	10.06±0.87	4.7	+35±10
	25-35	1.18±0.28	17.37±0.92	2.0	+25±4
	35+	0.38±0.18	66.87±19.27	0.6	-32±32
Extensive Thaw	0-5	9.88±3.38	3.06±0.76	14.0	+101±7
	5-15	4.26±1.38	5.13±1.90	12.2	+96±13
	15-25	2.05±1.01	8.80±0.79	4.7	+53±6
	25-35	1.98±0.58	14.61±3.14	2.0	+48±1
	35+	0.46±0.13	181.86±46.21	0.6	-56±66

Supplementary Table 5. Statistical partitioning estimates of the contribution of different respiration sources (plants, surface soil, deep soil) to total ecosystem respiration at monthly intervals during the growing season. Means ± (SD). The flux-weighted average is estimated for the full growing season (May-Sept).

		Plant			**Surface**			**Deep**		
		Min	Mod	Ext	Min	Mod	Ext	Min	Mod	Ext
2004	June	28±20	20±15	16±12	67±19	74±13	80±10	5±4	6±4	4±4
	July	45±27	40±24	40±24	42±23	28±17	28±17	13±7	33±12	32±10
	Aug	26±19	20±15	39±24	70±17	74±13	50±19	4±3	6±4	11±7
	Sept	22±16	17±12	28±19	74±15	78±11	65±16	4±3	5±4	8±6
	Av	**30±20**	**24±16**	**30±20**	**54±18**	**63±13**	**63±16**	**7±4**	**12±6**	**14±7**
2005	June	38±25	37±24	35±22	53±22	50±19	53±17	9±4	13±9	12±8
	July	23±17	27±19	37±23	71±15	64±16	50±18	5±7	10±7	13±8
	Aug	27±20	31±21	32±21	67±18	58±18	57±16	6±3	11±8	11±7
	Sept	45±27	41±26	44±26	42±22	43±20	40±19	14±3	16±10	16±9
	Av	**33±22**	**34±23**	**37±23**	**58±19**	**54±18**	**50±17**	**9±6**	**13±9**	**13±8**
2006	May	34±23	44±26	41±25	58±21	30±17	27±16	8±6	26±13	31±10
	June	40±26	41±26	37±23	51±22	43±19	51±17	10±7	16±10	12±8
	July	34±24	39±25	36±23	59±21	47±20	51±17	8±6	15±10	12±8
	Aug	32±22	42±26	36±22	62±20	40±19	23±14	7±5	18±11	41±10
	Sept	45±27	41±26	44±26	42±22	43±20	40±19	14±8	16±10	16±9
	Av	**37±24**	**41±26**	**39±24**	**54±21**	**40±19**	**39±17**	**9±6**	**18±11**	**23±9**

Supplementary Table 6. Two-pool mixing model estimate of the percent contribution of old C to winter respiration. Values are means ± (SE). Values were set to 100 when the observed field isotope measurements were lower than the deep soil end member value; this is a result of preferential freezing of surface soil layers during the winter, highlighting the contribution from deep soil.

	Minimal Thaw	Moderate Thaw	Extensive Thaw
Oct 2004	31.4±22.2	79.4±24.4	33.7±16.1
Nov 2006	66.3±17.1	93.2±32.9	75.2±15.6
Dec 2005	99.3±23.8	100 (NA)	73.6±16.9
Feb 2006	100 (NA)	100 (NA)	100 (NA)